Supplementary Information

Allosteric regulation of Glutamate dehydrogenase deamination activity

Soumen Bera[1], Mubasher Rashid[1], Gui-Quan Sun[2], Alexander B. Medvinsky[3], Bai-Lian Li[4], Claudia Acquisti[5], Adnan Sljoka[6,7], Amit Chakraborty[1*]

[1]School of Mathematics, Statistics and Computational Sciences, Central University of Rajasthan, Bandarsindri, Ajmer, India.

[2]Department of Mathematics, North University of China, Shanxi, China.

[3]Institute of Theoretical and Experimental Biophysics, Pushchino, Russia.

[4]University of California, Riverside, USA.

[5]Institute for Theoretical Biology, Humboldt University, Berlin, Germany.

[6]RIKEN Center for Advanced Intelligence Project, Tokyo, Japan.

[7]Department of Chemistry, University of Toronto, Canada.

*Corresponding author:
Amit Chakraborty
E-mail: amitc.maths@curaj.ac.in

Lead contact:
Amit Chakraborty
E-mail: amitc.maths@curaj.ac.in

| Helix No	Apo (Helix size)			NADH+GTP+GDH open (Helix size)			NADH+GTP+GDH closed (Helix size)			Correlation Coefficient(r)
	Residue Id	Length (Å)	Radius (Å)	Residue Id	Length (Å)	Radius (Å)	Residue Id	Length (Å)	Radius (Å)	
α1	8-29	33	2	8-32	35.5	2.4	8-30	34.1	2.3	0.79577
α2	38-53	25.2	1.8	39-53	23.5	1.9	37-53	25.7	1.9	
α3	100-115	23.6	1.9	100-118	28.1	1.9	100-118	27.6	1.9	
α4	139-154	24.9	1.9	139-155	26.1	1.8	139-155	26.1	1.8	
α5	172-184	19.7	1.9	172-184	19.6	1.9	172-187	23.2	2.0	
α6 (intermediate of pivotal, α8 and α9 helix)	213-237	32.6	2.7	213-224	19.2	1.8	213-237	32.2	2.7	0.25427
α7	--------			229-234	8.1	2.0	-----------			
α8	253-265	18.7	1.9	255-265	17.3	1.8	253-265	19.1	1.9	
α9	287-299	16.9	2.1	287-298	16.4	2.0	287-298	16.1	2.0	
α10	353-361	14.2	1.8	353-363	16.1	1.8	353-363	15.9	1.9	
α11 (elongated helix)	376-391	23.5	1.9	369-388	31.5	2.0	369-388	31.2	2.0	
α12 (Antenna helix)	398-425	38.7	2.4	398-407	15.9	1.8	398-425	42.2	2.3	0.21784
α13 (Antenna helix)	---------			409-421	19.3	1.8	----------			
α14 (Antenna helix)	434-442	13.1	1.9	433-442	13.6	2.0	433-439	10	1.9	
α15 (pivot helix)	444-471	42.1	1.9	444-471	42.2	1.9	444-471	41.1	1.9	0.79394
α16	476-497	33.3	1.9	476-497	33.2	1.9	476-496	33.1	1.9	0.03860

Supplementary table 1: Detail information of helices. Table represents helix number, helix length, radius and corresponding correlation coefficient (r) compare with the open structure. Helix number is introduced from Stride Services (Heinig et al.,2004). Helix length and radius is calculated from Chimera software. Low deviation correlation coefficient indicates the lack of similar pattern between helices (open to closed). Table indicates α1- α5 and α15 have high level of correlation compare to helices α6 to α11 and Antenna helices. In contrast, the table suggest a lack of similarity in NBD (α6 – α11) and Antenna region indicates helical rotation and translation.

**Notes: Deviation of Cα atoms:**

Cα deviation movement is measured using formula:

$$\sqrt{\frac{1}{n}\sum_1^n((x_i - x_0)^2 + (y_i - y_0)^2 + (z_i - z_0)^2)}\,,$$

where (x_i, y_i, z_i) are the position of the Cα atoms of every residue within GDH (3jd3 open and 3jd4 closed). The deviation is measured in all cases from unbound GDH structure (3jcz). Deviation is compaired and visualize with different conformation of GDH using small code of Python. Helix number also included with this comparison to understand the region of changes in deformation of Cα atom between different conformations of GDH.
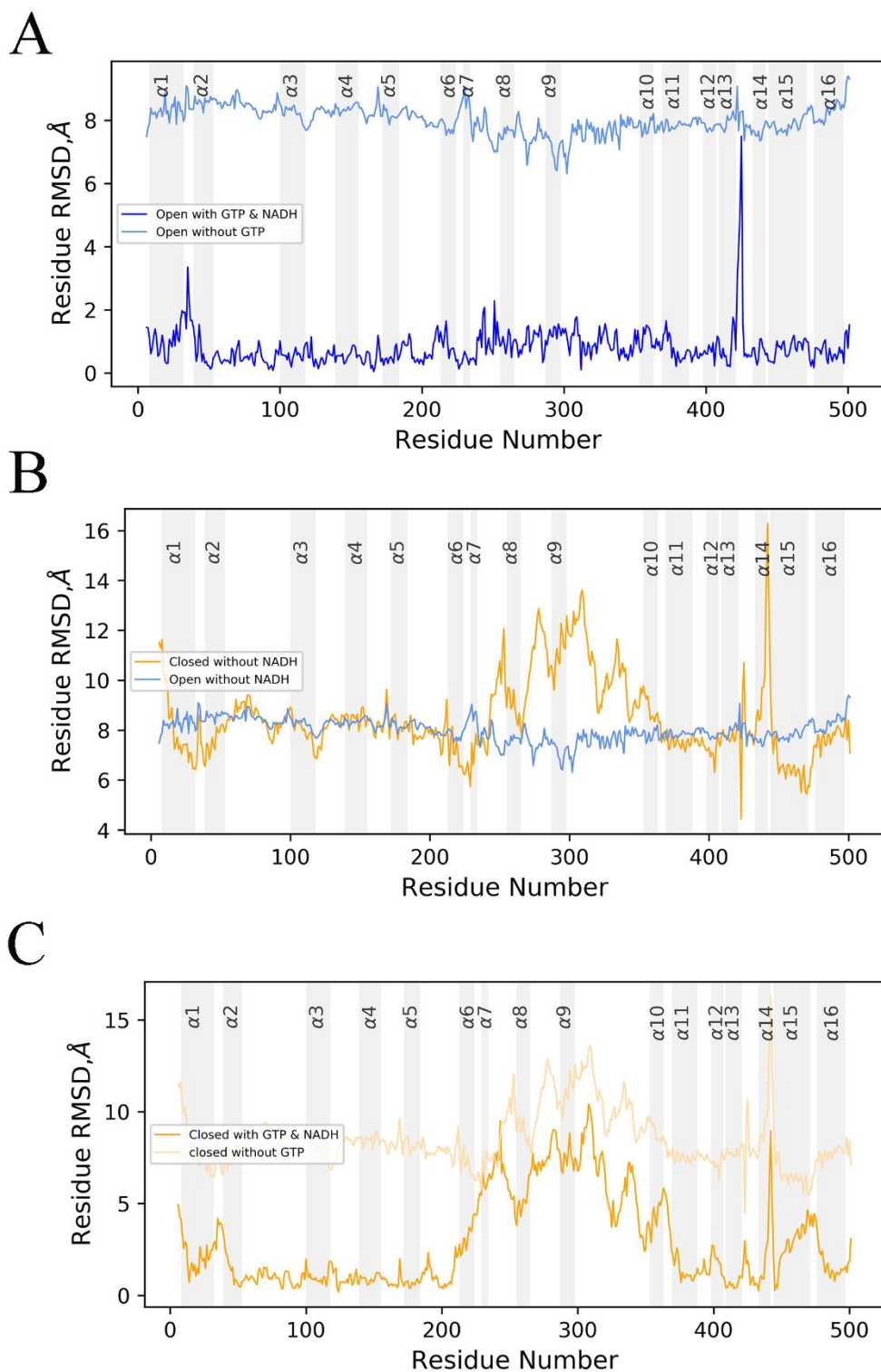
Supplementary figure 1: Compare of Cα deviation. Figure showing the individual Cα deviation of different structures (GDH with NADH closed, GDH with NADH open, GDH with NADH and GTP open, GDH with NADH and GTP closed) superimposing with Apo structure (GDH only). (A) Plot indicates the effects of GTP on open structures (B) Figure also indicates the effects of GTP on open as well as closed structure (GDH with NADH open and GDH with NADH closed). (C) Plot compares individual residue deviation between closed structures with and without GTP. Helices are indicated with shaded region and all the figure is generated using Python code.
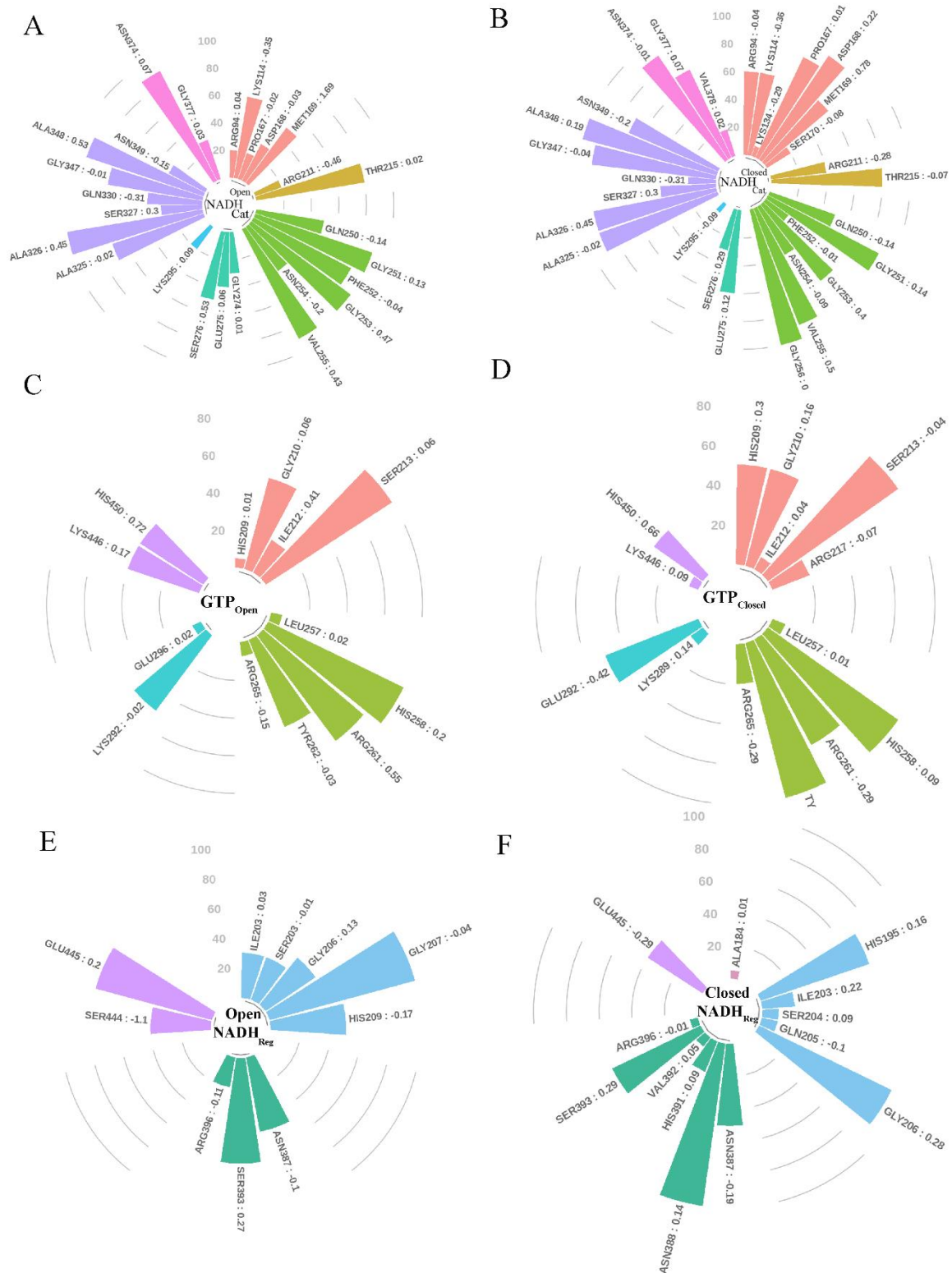
Supplementary figure 2: Interaction between cofactors NADH, inhibitor GTP with GDH. Plot showing detail information of interfaces residues with ligands at two different conformations (open and closed). Group wise colours designates with alpha helices or outside of alpha helices. Each bar represents the contribution of buried surface area (BSA) of interfacing residues with ligands and fraction numbers at top of the head of each bar showing solvation energy effect ($\Delta^{i}G$ Kcl/mol). (A), (B) figure showing the interaction between

interface residue of protein and catalytic NADH at open and closed confirmation. Number of interfacing residues (29) in closed conformation much higher than open (26) at catalytic site. Medium purple colour bars indicate the residue in NBD domain but not in alpha helices however violate and lime green bars situated at α11 and α8 respectively. (C), (D) represents the interfacing residues of protein with GTP. Percentage of buried surface area of His 209, Arg261 and Tyr 262 are sufficient increased in closed structure compare to open indicate
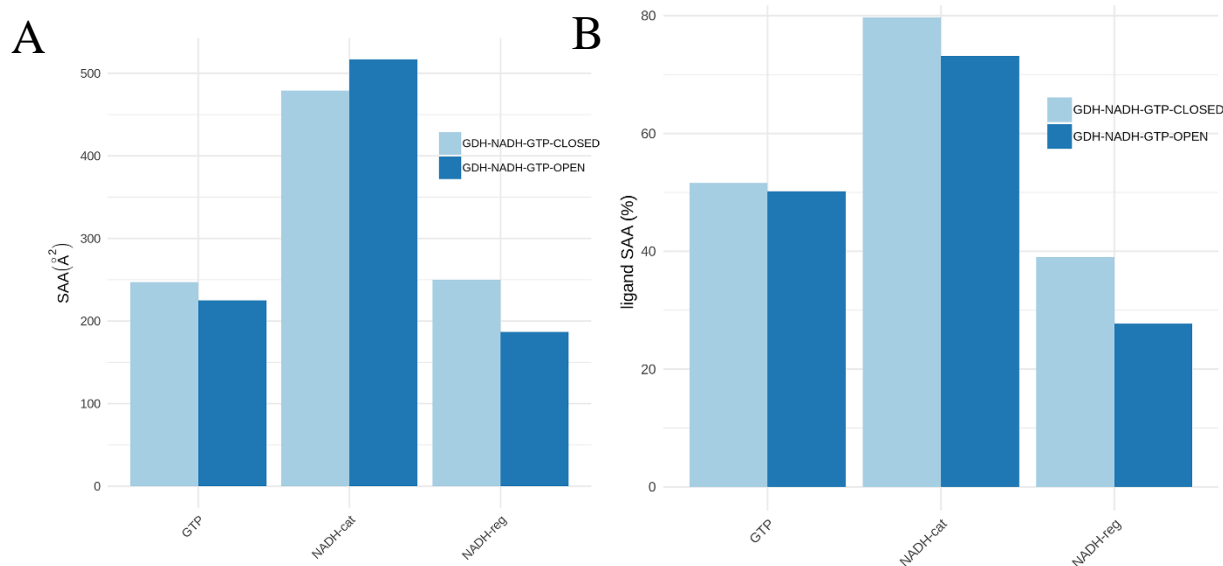
Supplementary figure 3: Solvent Accessible Area (SAA) of protein and ligand in-between the protein ligand interfaces. (A) figure represents Solvent Accessible Area (SAA) of protein interfaces between GTP, NADH catalytic and NADH regulatory site however figure (B) showing the SAA (%) of GTP, NADH catalytic and NADH regulatory between protein. The solvent accessibility of protein at NADH catalytic site is significantly higher for open structures indicates the flexibility of protein at catalytic site compare to closed one.

(A) 3jd3 open structure: Interface

Structure1				Structure2				Interface Area($Å^2$)	ΔG Kcl/mol	N_{HB}
Range	N_{at}	N_{res}	Surface ($Å^2$)	Range	Nat	Nres	Surface ($Å^2$)			
Chain A	73	28	23318	NAI: Catalytic	42	1	825	560.0	-7.8	8
Chain C	30	10	23318	NAI: Regulatory	20	1	773	200.8	-1.9	2
Chain A	34	13	23318	GTP	24	1	540	248.0	-5.4	3

(A) 3jd4 closed structure: Interface

Structure1				Structure2				Interface Area($Å^2$)	ΔG Kcl/mol	N_{HB}
Range	N_{at}	N_{res}	Surface ($Å^2$)	Range	Nat	Nres	Surface ($Å^2$)			
Chain A	80	31	22631	NAI: Catalytic	43	1	802	559.2	-6.4	8
Chain A	40	14	22631	NAI: Regulatory	28	1	829	286.9	-3.4	2
Chain A	34	14	22631	GTP	26	1	573	271.4	-1.4	7

Supplementary table 2: Comparison between protein and ligand interfaces. The above table Structure1 represent GDH and Structure2 represent cofactors NADH and inhibitor GTP. N_{at}, N_{res} indicate number of atoms and number of residues involved in interface area between protein and cofactors as well as inhibitor. N_{HB} indicates no of hydrogen bonds present at interfaces and ΔG (Kcl/mol) is solvation energy for folding. All information were extracted from PDBePISA (https://www.ebi.ac.uk/pdbe/pisa/).

A **Catalytic NADH interface: Hydrogen bonds**

No	Structure1	Dist (Å)	Structure2
1	A: ASN 254 [N]	2.92	A: NAI 602 [O2A]
2	A: PHE 252 [N]	2.88	A: NAI 602 [O3B]
3	A: GLY 253 [N]	3.11	A: NAI 602 [O3B]
4	A: SER 276 [N]	2.47	A: NAI 602 [O2B]
5	A: ASN 254 [N]	2.76	A: NAI 602 [O3]
6	A: ASN 254 [ND2]	3.03	A: NAI 602 [O2N]
7	A: THR 215 [OG1]	3.89	A: NAI 602 [O7N]
8	A: GLN 250 [O]	3.61	A: NAI 602 [N3A]

B **Catalytic NADH interface: Hydrogen bonds**

No	Structure1	Dist (Å)	Structure2
1	A: SER 170 [N]	2.92	A: NAI 601 [O1A]
2	A: ASN 254 [N]	3.26	A: NAI 601 [O2A]
3	A: ASN 254 [N]	3.68	A: NAI 601 [O3]
4	A: ASN 254 [ND2]	3.54	A: NAI 601 [O2N]
5	A: ARG 94 [NH2]	3.85	A: NAI 601 [O3D]
6	A: ASN 349 [N]	3.78	A: NAI 601 [O2D]
7	A: ARG 94 [NH2]	3.03	A: NAI 601 [O2D]
8	A: ASN 349 [ND2]	2.45	A: NAI 601 [O2D]

Regulatory NADH interface: Hydrogen bonds

No	Structure1	Dist (Å)	Structure2
1	A: SER 444[OG]	3.40	C: NAI 601[O3D]
2	A: HIS 209[NE2]	3.84	C: NAI 601[O2D]

Regulatory NADH interface: Hydrogen bonds

No	Structure1	Dist (Å)	Structure2
1	A: VAL 392[N]	3.36	C: NAI 603[O3D]
2	A: HIS 195[NE2]	3.32	C: NAI 603[O2D]

Supplementary table 3: Identifying hydrogen bond corresponding amino acids involved in NADH interfaces. Figure A represent the closed GDH-GTP-NADH structure and figure B represent open GDH-GTP-NADH structure. The number of hydrogen bonds at NADH interfaces are same in both the condition however there are significantly changes in amino acids and corresponding hydrogen bond distances (Å). Moreover, in closed situation, catalytic NADH showing stronger interaction with NBD domain (all the hydrogen bond formation amino acid belongs to NBD domain).

A **GTP binding: Hydrogen bonds**

No	Structure1	Dist (Å)	Structure2
1	A: ARG 265 [NH1]	3.60	A: GTP 602 [O1G]
2	A: ARG 265 [NH1]	3.53	A: GTP 602 [O2G]
3	A: TYR 262 [OH]	2.35	A: GTP 602 [O3G]
4	A: HIS 209 [NE2]	2.36	A: GTP 602 [O2B]
5	A: SER 213 [OG]	2.75	A: GTP 602 [O2]
6	A: GLU 292 [OE1]	3.43	A: GTP 602 [N1]
7	A: GLU 292 [OE2]	2.72	A: GTP 602 [N2]

B **GTP binding: Hydrogen bonds**

No	Structure1	Dist (Å)	Structure2
1	A: ARG 261 [NH2]	2.78	A: GTP 601 [03G]
2	A: TYR 262 [OH]	2.84	A: GTP 601 [O3G]
3	A: HIS 450 [NE2]	3.23	A: GTP 601 [O1B]

C **GTP without NADH: Hydrogen bonds**

No	Structure1	Dist (Å)	Structure2
1	A: SER 213 [OG]	3.88	A: GTP 601 [O1G]
2	A: ARG 261 [NE]	2.74	A: GTP 601 [O3G]
3	A: ARG 265 [NH2]	3.20	A: GTP 601 [O3G]
4	A: ARG 261 [NH2]	2.71	A: GTP 601 [O3G]
5	A: GLU 292 [OE2]	3.13	A: GTP 601 [N1]

Supplementary table 4: Identifying hydrogen bond corresponding amino acids involved in GTP interfaces. Table A and B represent hydrogen bond with GTP in closed and open structure. Table C represent number of hydrogen bonds with GTP in GDH-GTP without NADH structure. So, in closed structure showing high volume of hydrogen bonds compare to open and GDH-GTP without NADH structure indicates stronger interaction of GTP with GDH in closed situation.
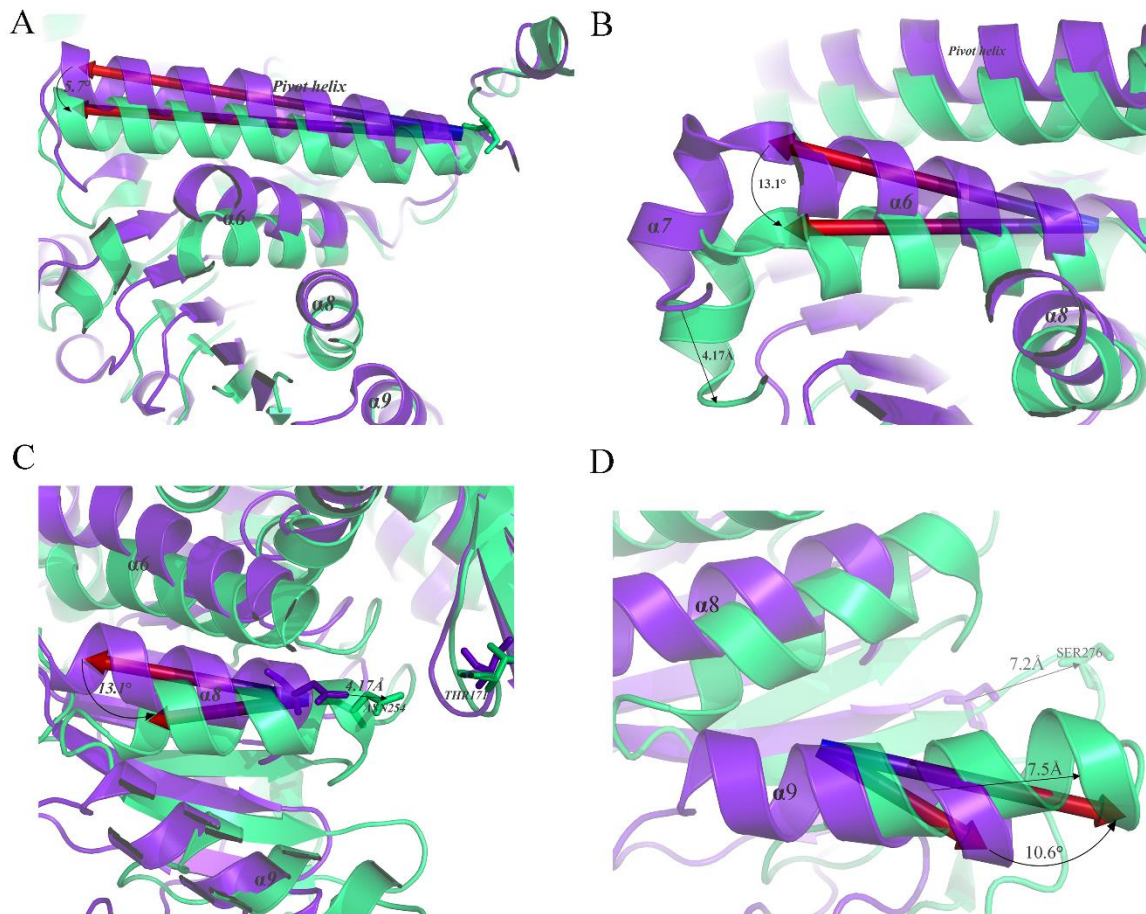
Supplementary figure 4: **Translation and rotation of superimposed helices** (open as purple and closed as lime green) those are situated at significantly high RMSD position (200 to 390) within protein. Pivotal and α6 helices is rotated (5.7° and 13.1°) antilock wise however according to figure C and D, α8 and α9 helices is rotated (13.1° and 10.6°) as well as translated (4.75Å and 7.5Å) towards catalytic site. This translation as well as rotation indicate the shifting (Ser276 is shifted approx. 7.2Å) of NBD domain towards catalytic site and closed the catalytic cleft. All the figure above is generated by UCSF Chimera.

| Number of mutations	Amino acid change in mature enzyme	"Sporadic"/ "Familial"	Exons	Positions in structure
1	SER ⟶ Cys at 213	0/1	6 and 7	4 Å of GTP
12	Arg ⟶ Cys at 217	3/9	6 and 7	4 Å of GTP
2	His ⟶ Thr at 258	2/0	6 and 7	4 Å of GTP
2	Arg ⟶ Thr at 261	2/0	6 and 7	4 Å of GTP
1	Arg ⟶ Ser at 261	0/1	6 and 7	4 Å of GTP
1	Tyr ⟶ Cys at 262	1/0	6 and 7	4 Å of GTP
1	Tyr ⟶ His at 262	1/0	6 and 7	4 Å of GTP
13	Arg ⟶ His at 265	2/11	6 and 7	4 Å of GTP
1	Arg ⟶ Cys at 265	1/0	6 and 7	4 Å of GTP
1	Leu ⟶ Val at 409	1/0	10,11 and 12	Antenna
2	Asn ⟶ Tyr at 406	2/0	10,11 and 12	Antenna
1	Phe ⟶ Leu at 436	1/0	10,11 and 12	Antenna
1	Gln ⟶ Arg at 437	1/0	10,11 and 12	Antenna
4	Gly ⟶ Val at 442	4/0	10,11 and 12	Antenna
3	Gly ⟶ Asp at 442	3/0	10,11 and 12	Antenna
3	Gly ⟶ Ser at 442	3/0	10,11 and 12	Antenna
1	Gly ⟶ Cys at 442	1/0	10,11 and 12	Antenna
1	Gly ⟶ Arg at 442	1/0	10,11 and 12	Antenna
25	Ser ⟶ Leu at 441	24/1	10,11 and 12	Antenna
1	Ala ⟶ Thr at 443	0/1	10,11 and 12	Antenna
3	Ser ⟶ pro at 444	0/3	10,11 and 12	Pivotal
2	Lys ⟶ Glu at 446	1/1	10,11 and 12	Pivotal
2	His ⟶ Tyr at 450	1/1	10,11 and 12	Pivotal

Supplementary table 5: Mutational hotspots region. This table shows the location and frequency of hyperinsulinism–hyperammonemia syndrome (HI/HA) mutation in GDH. Out of total 84 cases, 66% is sporadic and 34% were Familial (Stanley et al., 2011). The table also indicate three mutational hotspot regions within protein, like GTP binding, Antenna and Pivotal helices region, however the highest number of mutations in HI/HA cashes has been observed at Leu441 whose position in the junction of pivotal and Antenna helices. Another position of mutation is His265 whose frequency also significantly higher in HI/HA cases.

| Structure ID	Hydrogen bond energy strength	Highest size rigid cluster	Participating helices (%, towards N or C terminal) within rigid cluster	Total No of Rigid Cluster	Independent DOF	No of hydrogen bond	Independent Hinge joint
3jczA (Open)	0.0	5274	$\alpha1(91,N),\alpha2(93,C),\alpha3,\alpha4,\alpha5,\alpha6\&\alpha7(0.87,C)$ $\alpha8(67,C),\alpha9(92,N),\alpha10,\alpha11(93,N),\alpha15,\alpha16(90,N)$	1264	614	393	476
	0.5	4791	$\alpha1(86,N),\alpha2(33,C),\alpha3,\alpha4,\alpha5,\alpha6\&\alpha7(87,C)$ $\alpha8(67,C),\alpha10,\alpha11(93,N),\alpha15,\alpha16(90,N)$	1448	663	349	506
	1	1867	$\alpha4(20,N),\alpha5,\alpha6\&\alpha7(83,C),\alpha8(67,C),\alpha10,\alpha15,$ $\alpha16(67,N)$	2265	740	297	544
	1.5	1362	$\alpha6\&\alpha7(45,N\&C),\alpha8(67,C),\alpha10,\alpha16(52,N)$	2721	836	251	567
	2	805	$\alpha6\&\alpha7(45,N\&C),\alpha8(67,C)$	3009	909	220	585
3jd3A (Open)	0.0	4809	$\alpha1,\alpha2,\alpha3,\alpha4,\alpha6\&\alpha7(95,C),\alpha8,\alpha9(73,N),\alpha10(70,N)$ $\alpha11,\alpha15,\alpha16(90,N)$	1389	669	376	506
	0.5	2846	$\alpha1(96,N),\alpha6\&\alpha7(95,C),\alpha8,\alpha9(73,N),\alpha10(70,N)$ $\alpha11(33,N),\alpha15,\alpha16(90,N)$	1935	725	324	536
	1	1471	$\alpha6\&\alpha7(83,C),\alpha8,\alpha9(64,N),\alpha15(92,C)$	2479	809	280	570
	1.5	1025	$\alpha6\&\alpha7(62,C),\alpha8,\alpha9(64,N)$	2690	895	236	588
	2.0	232	$\alpha6\&\alpha7(38,C)$	3207	1017	190	618
3jd4A (Closed)	0.0	5580	$\alpha1(96,N),\alpha2,\alpha3(94,C),\alpha4,\alpha5,\alpha6\&\alpha7,\alpha8,\alpha9$ $\alpha10,\alpha11(95,N),\alpha15(67,C),\alpha16(92,N)$	1167	617	412	484
	0.5	5121	$\alpha1(96,N),\alpha2,\alpha3(94,C),\alpha4,\alpha5,\alpha6\&\alpha7(96,C),\alpha8$ $\alpha9(75,N),\alpha10,\alpha11(84,N),\alpha15(66,C),\alpha16(92,N)$	1355	670	363	511
	1	4784	$\alpha1(96,N),\alpha2,\alpha3(94,C),\alpha4,\alpha5,\alpha6\&\alpha7(96,C),\alpha8$ $\alpha9(75,N),\alpha10,\alpha11(84,N),\alpha15(66,C),\alpha16(92,N)$	1499	719	317	537
	1.5	1748	$\alpha3(94,C),\alpha4,\alpha5(92,N),\alpha11(43,N)$	2478	803	270	551
	2	652	$\alpha4(87,N)$	2908	903	226	580

Supplementary table 6: Details table of rigidity based allosteric transmission using ProFlex/FIRST. Hydrogen bond energy strength is considered from 0 to -2.0 as communication is started after hydrogen bond cut off 0.0 and has been stopped before cut-off -1.5 (supplementary figure). The table also indicated the position and percentage of helices those are involved with in rigid cluster at different hydrogen bond energy cut-off.

A
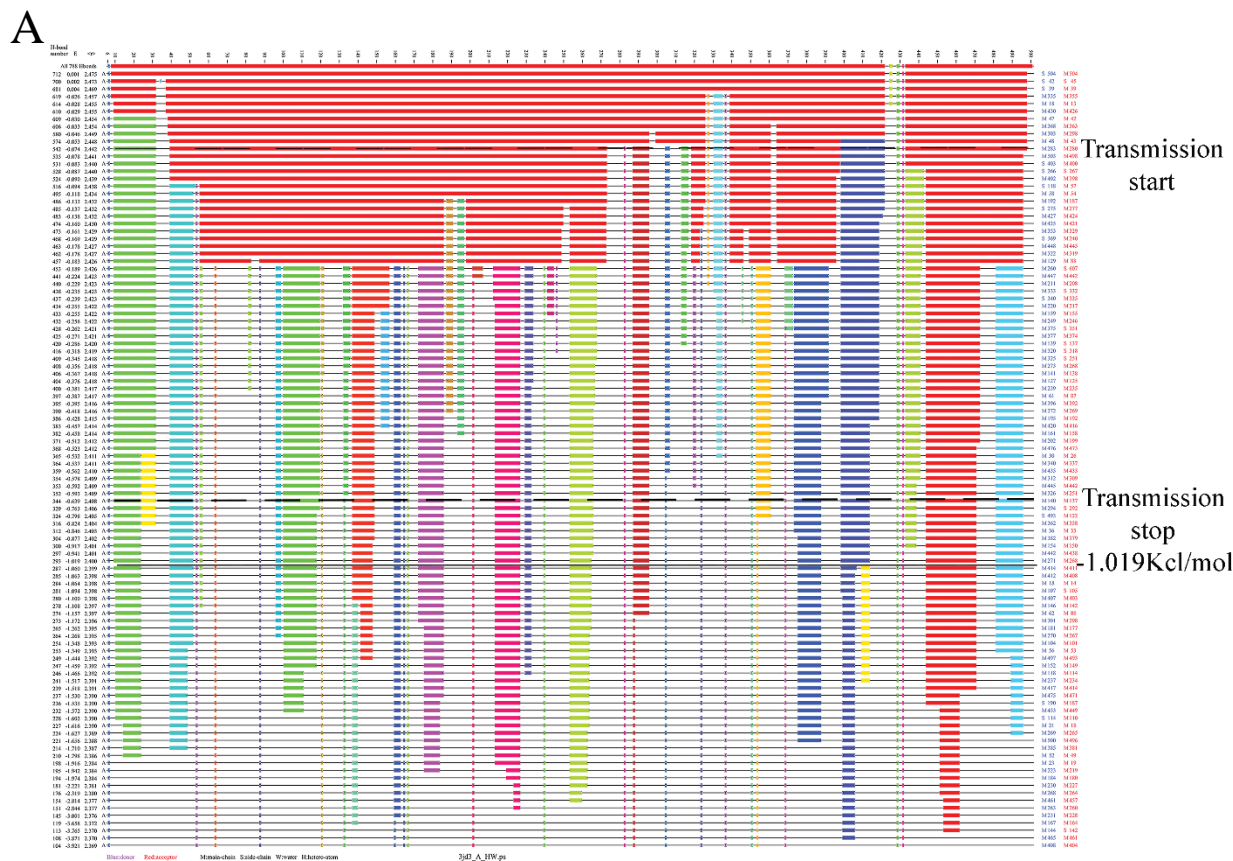
B
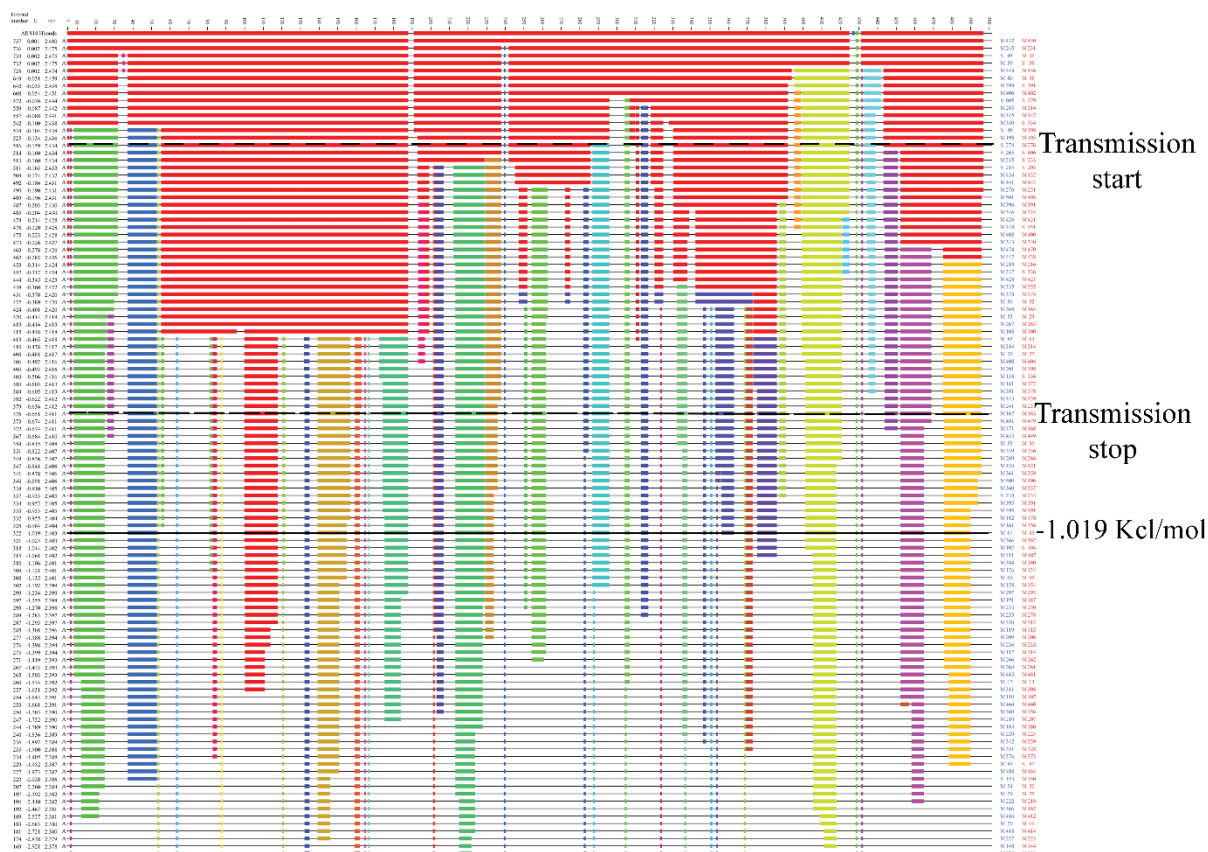
Supplementary figure 5: **Hydrogen bond dilution plot.** (A), (B) Dilution plot of GDH open (PDB ID 3jd3) and GDH closed (PDB ID 3jd4) using ProFlex / FIRST (Jacobs et al., 2001). Horizontal axis represents residue numbers and vertical axis represent hydrogen bond energy cut off (Kcl/mol). Protein flexibility shows by horizontal grey lines however solid colour lines indicate rigid cluster at different hydrogen bond energy cut off. Last two column (blue and red) represent hydrogen donor and acceptor respectively. Black dotted lines (upper and lower) indicates allosteric communication start and stop associated hydrogen bond energy cut off.
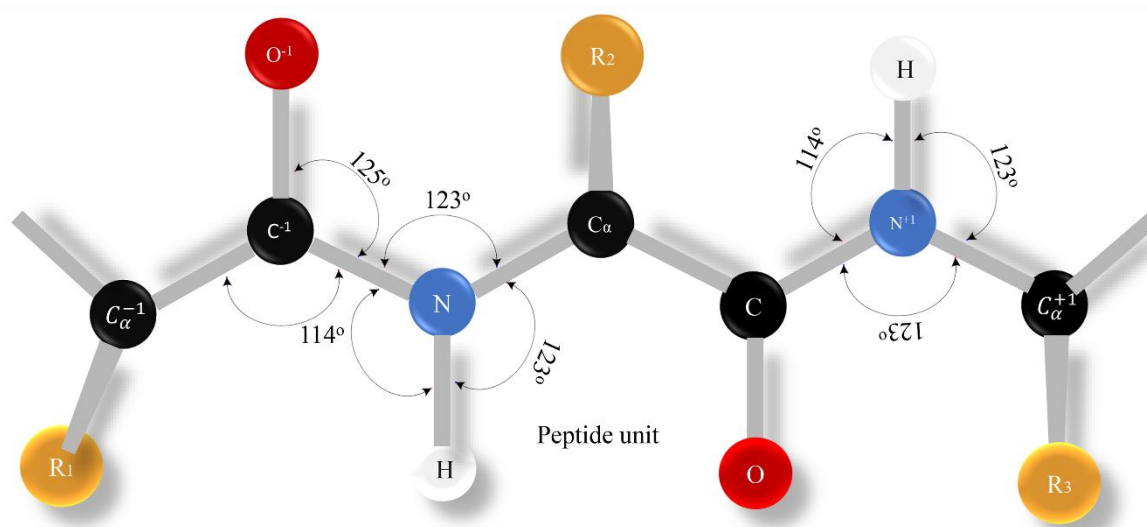
Supplementary figure 6: Structural description of peptide chain geometry i.e. amino acids in proteins (or polypeptides) are joined together by peptide bonds. R_1, R_2 and R_3 group represent the side chain of each amino acid.
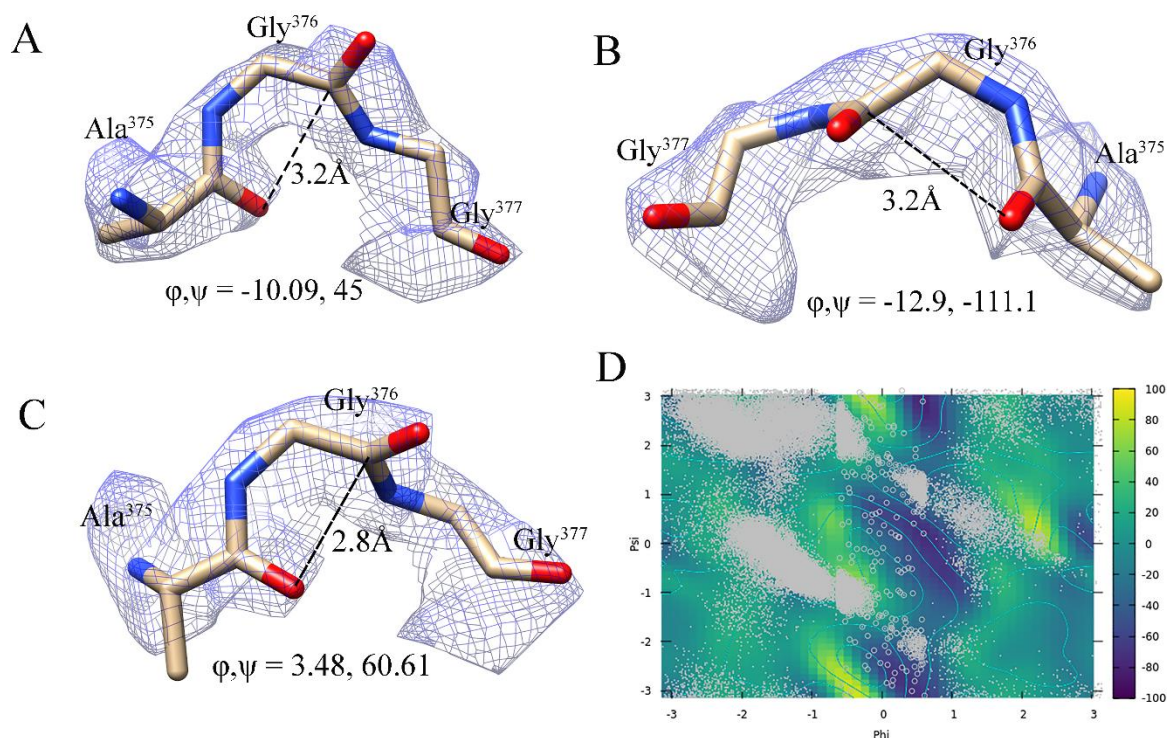
Supplementary figure 7: **Residue reliability and populated high-energy pass in transition upon mutation.** Figure (A), (B) and (C) showing the evidence of density map for a reliable residue at different time of trajectory (0.4ns, 9.3ns and 4ns) by adopting a confirmation at $-35 < \varphi < 35$. The residues Ala375, Gly376 and Gly377 from pdb snapshot at different time step (0.4ns, 9.3ns and 4ns) fitted with EM maps by chimera tool. Dotted black lines within figure is showing O^{-1} …C distance corresponding to φ, ψ angles at different conformational states. (D) φ, ψ angles describing the local conformation changes of mountain pass residues at different time point trajectory after 10ns MD simulation upon mutant GDH structure (Gly376Asp). The zoomed circle indicates the position of transient residues at conformation $-35 < \varphi < 35$. Colour gradient also specifies the region of free energy landscape of Gly376 upon mutilation by Asp.
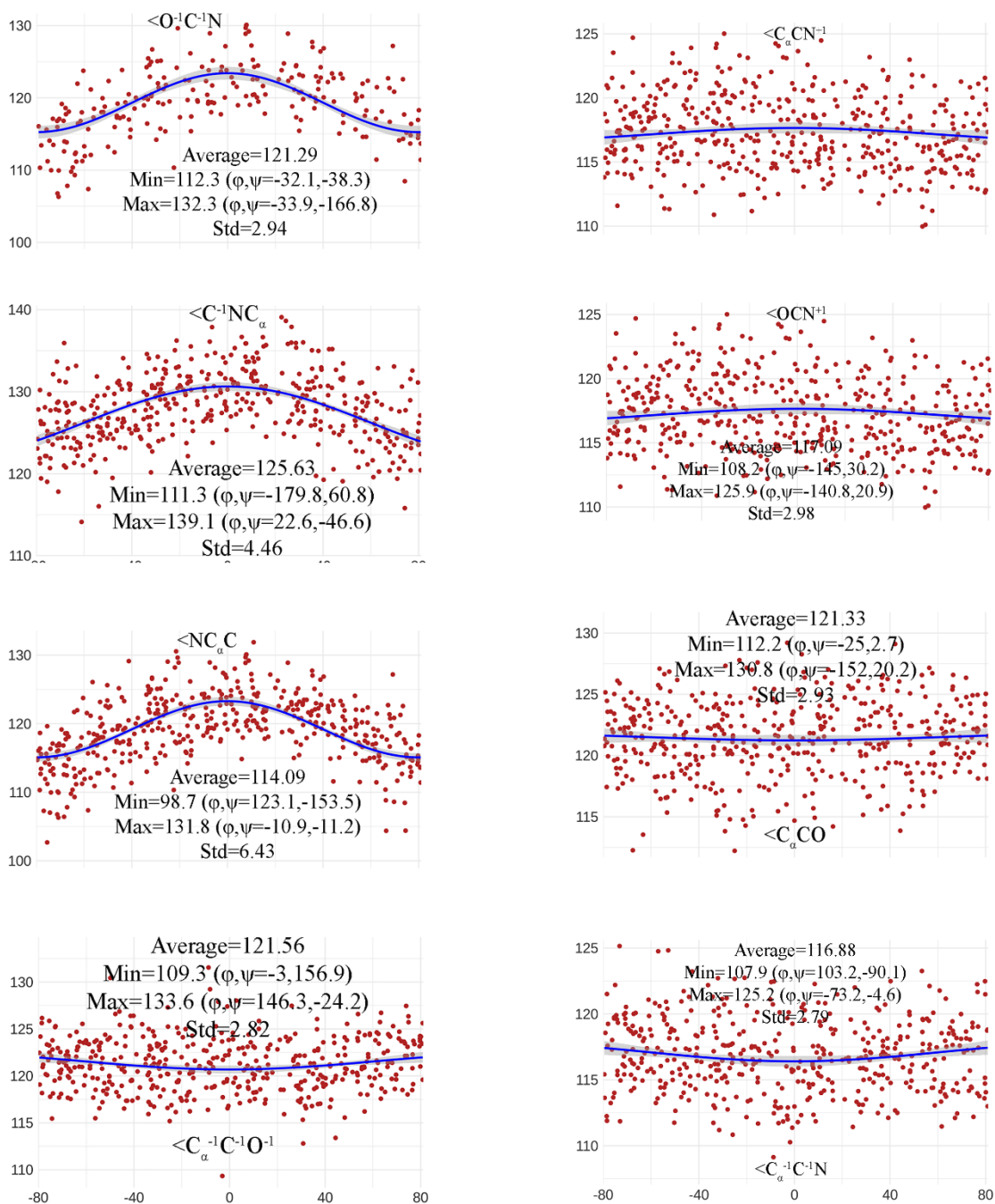
Supplementary figure 8: Deformation of geometry with transition at high-energy pass. Bond angle variations by obtaining the $\varphi \leq 0^o$ and $\varphi \geq 0^o$ transitions based on the MD trajectory data. Blue lines represent calculated fits of observed MD trajectory data using cosine equations to describe the systematic distortion of bond angles.
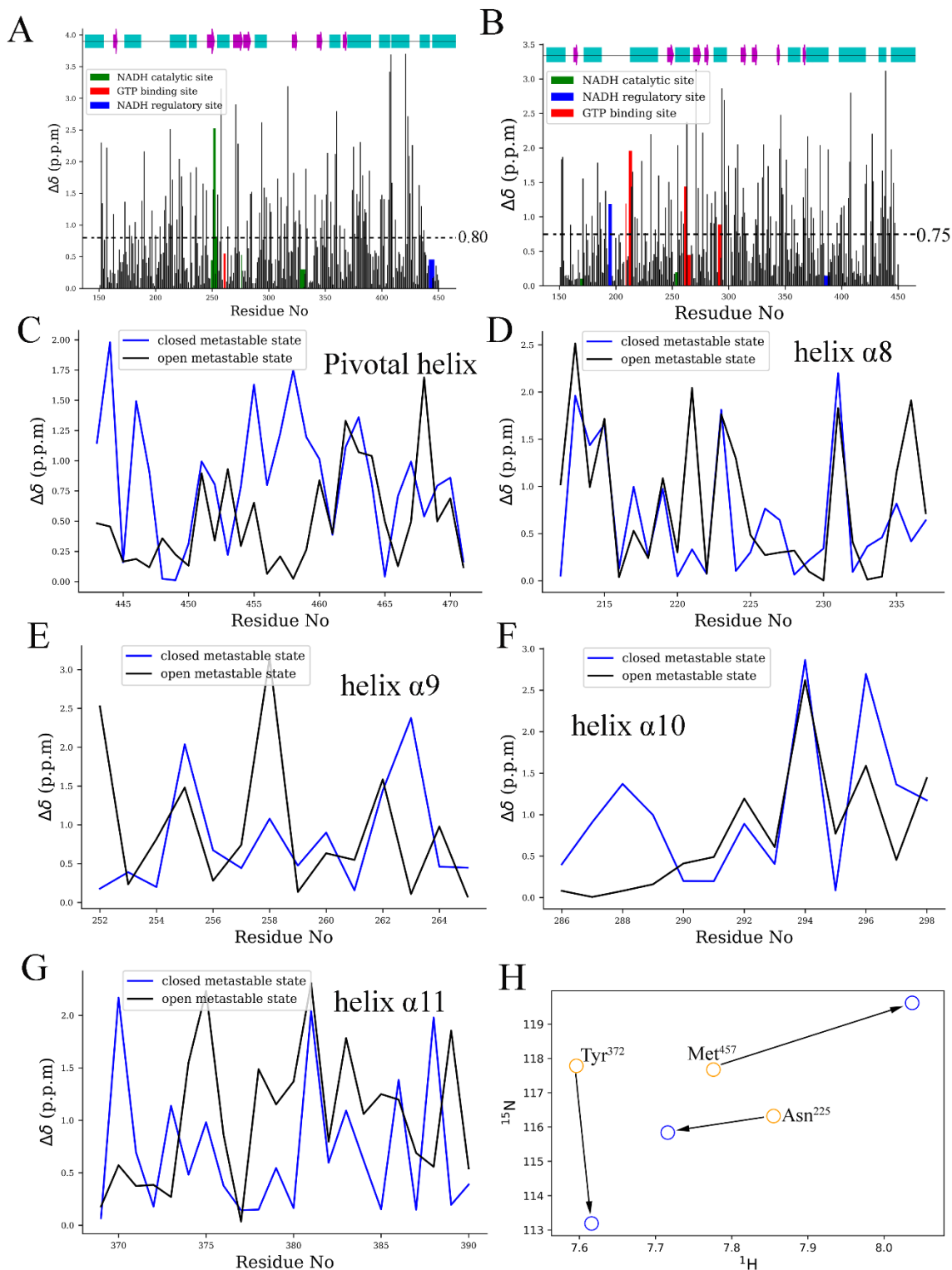
Supplementary figure 9: Computation prediction of chemical shift. Comparison of Chemical Shift between open and closed conformations was predicted by SHIFTX2 software (Han et al., 2011). (A) figure shows the difference of chemical shift in-between Apo (3jcz)

and NADH-GTP open (3jd3) structure. Colour area indicated the binding site of GTP and NADH. Top of the figure, rectangle and arrow with filled cyan and magenta colours mapped with alpha helices and beta sheets to indicate position of the residue. The dotted black line shows the average value of difference chemical shift (in ppm). (B) this figure also shows the difference chemical shift between Apo and NADH-GTP closed (3jd4) structures. Here the average chemical shift difference (in ppm) is slightly lower than former one. (C) figure shows 13CA chemical shift difference of pivotal helix where back and blue line represents NADH-GTP open and NADH-GTP closed structures. (D), (E), (F) and (G) also shows the 13CA chemical shift differences of α8, α9, α10 and α11 respectively. (H) 15N − 1H chemical shift differences of Tyr 372, Met 457 and Asn 225 indicates the loss of hydrogen bond in open structure (figure 2). All data were generated by SHIFTX2 (http://www.shiftx2.ca/) using experimental pH and temperature(K) available in PDB data (Han et al., 2011).

Reside ID &NO	Frequency >=10	Position
ALA-194	12	Regulatory
ALA-341	31	coenzyme binding domain
ALA-375	22	Catalytic&376
ALA-443	91	Regulatory
ASN-254	20	Catalytic
ASP-119	17	--------
GLU-25	42	--------
GLU-328	49	Catalytic
GLU-36	19	--------
GLY-243	68	coenzyme binding domain
GLY-350	53	Catalytic
GLY-376	197	Catalytic
GLY-377	19	Catalytic
HIS-189	24	Regulatory
HIS-209	31	Regulatory
LEU-371	14	coenzyme binding domain and alpha11
LYS-329	28	Catalytic
MET-169	63	Catalytic
PHE-122	84	---------
PHE-304	10	coenzyme binding domain
PRO-165	39	Catalytic
PRO-167	40	Catalytic
PRO-202	21	Regulatory
PRO-240	32	coenzyme binding domain
PRO-288	16	coenzyme binding domain
PRO-354	19	coenzyme binding domain
PRO-432	82	Antenna
PRO-7	56	N-terminal
PRO-88	15	-------
SER-327	33	--------
SER-393	41	Regulatory
THR-34	18	--------
THR-37	36	--------

Reside ID &NO	Frequency >=10	Position
THR-427	14	Antenna
VAL-99	19	Catalytic

Supplementary table 7: Frequency of amino acids in the high-energy transition region. All the amino acid residues with frequency higher than 10 and fall into the region -35 < φ < 35 were taken after 10ns MD simulation upon GDH structure. Cyan colour indicates the frequency of Gly376 and its neighbourhood residues.

Reside ID &NO	Frequency >=10	Position
ALA-336	10	coenzyme binding domain
ALA-341	43	coenzyme binding domain
ALA-434	25	antenna
ARG-211	36	GTP binding area
ARG-396	15	regulatory
ASP-119	47	------
ASP-138	12	------
ASP-370	18	coenzyme binding domain and alpha11
ASP-376	168	catalytic
GLU-173	25	catalytic
GLU-25	60	------
GLU-36	33	------
GLU-38	13	------
GLY-243	47	coenzyme binding domain
GLY-350	147	catalytic
GLY-377	16	catalytic
GLY-422	34	antenna
GLY-442	20	regulatory
ILE-203	11	regulatory
LEU-371	251	coenzyme binding domain and alpha11
LYS-329	26	------
LYS-53	20	------
MET-169	162	catalytic
PHE-304	20	coenzyme binding domain
PHE-9	18	N-terminal
PRO-165	116	catalytic
PRO-202	56	regulatory
PRO-240	30	coenzyme binding domain
PRO-354	17	catalytic
PRO-429	43	antenna
PRO-432	45	antenna
PRO-7	40	N-terminal
SER-276	58	coenzyme binding domain
SER-279	20	coenzyme binding domain

SER-393	41	regulatory
SER-83	19	None
VAL-378	24	catalytic

Supplementary table 8: Frequency of amino acids in the high-energy transition region upon mutation. Amino acid residues with frequency more than 10 and falling in the high energy region -35 < φ < 35 were selected after 10ns MD simulation upon mutated GDH structure Gly376Asp. Gly376 and its neighbourhood residues were highlighted in cyan colour showing less frequency compared to previous table.

References

Han, B. Liu, Y., Ginzinger, S. and Wishart, D. SHIFTX2: significantly improved protein chemical shift prediction. Journal of Biomolecular NMR, Volume 50, Number 1, 43-57 (2011).

Heinig, M., Frishman, D. STRIDE: A Web server for secondary structure assignment from known atomic coordinates of proteins. Nucl. Acids Res., 32, W500-2, (2004).

Jacobs, D. J., Rader, A. J., Kuhn, L. A. & Thorpe, M. F. Protein flexibility predictions using graph theory. Proteins 44, 150–165 (2001).

Jacobs, D. J., Rader, A. J., Kuhn, L. A. and Thorpe, M. F. Protein Flexibility Predictions Using Graph Theory (pdf) Proteins: Structure, Function, and Genetics, 44, 150-165 (2001).

Marsh J. A. Buried and Accessible Surface Area Control Intrinsic Protein Flexibility. J Mol Biol. 425(17), 3250-3263 (2013).

Stanley, C.A. Two genetic forms of hyperinsulinemic hypoglycaemia caused by dysregulation of glutamate dehydrogenase. Neurochemistry International. 59, 465-472 (2011).

Stanley, C.A., Lieu, Y.K., Hsu, B.Y., et al. Hyperinsulinism and hyperammo-nemia in infants with regulatory mutations of the glutamate dehydrogenase gene. N. Engl. J. Med. 338, 1352–1357 (1998).